ISSN 1674-1056
http://cpb.iphy.ac.cn
http://iopscience.iop.org/cpb
中国物理 B
Chinese Physics
中国物理
Chinese Physics B

One-dimensional mass transport with dynamic external potentials

Xingxing Zhang(张星星), Dongqin Zheng(郑冬琴), Weirong Zhong(钟伟荣)

Citation: Chin. Phys. B . 2019, 28(2): 020505. **doi:** 10.1088/1674-1056/28/2/020505
Journal homepage: http://cpb.iphy.ac.cn; http://iopscience.iop.org/cpb

What follows is a list of articles you may be interested in

Collective transport of Lennard–Jones particles through one-dimensional periodic potentials

Jian-hui He(何健辉), Jia-le Wen(温家乐), Pei-rong Chen(陈沛荣), Dong-qin Zheng(郑冬琴), Wei-rong Zhong(钟伟荣)
Chin. Phys. B . 2017, 26(7): 070502. **doi:** 10.1088/1674-1056/26/7/070502

Collective diffusion in carbon nanotubes: Crossover between one dimension and three dimensions

Pei-Rong Chen(陈沛荣), Zhi-Cheng Xu(徐志成), Yu Gu(古宇), Wei-Rong Zhong(钟伟荣)
Chin. Phys. B . 2016, 25(8): 086601. **doi:** 10.1088/1674-1056/25/8/086601

Molecular dynamics simulation of nanoscale surface diffusion of heterogeneous adatoms clusters

Muhammad Imran, Fayyaz Hussain, Muhammad Rashid, Muhammad Ismail, Hafeez Ullah, Yongqing Cai, M Arshad Javid, Ejaz Ahmad, S A Ahmad
Chin. Phys. B . 2016, 25(7): 076601. **doi:** 10.1088/1674-1056/25/7/076601

Normal thermal conduction in lattice models with asymmetric harmonic interparticle interactions

Zhong Yi, Zhang Yong, Wang Jiao, Zhao Hong
Chin. Phys. B . 2013, 22(7): 070505. **doi:** 10.1088/1674-1056/22/7/070505

Novel loop-like solitons for generalized Vakhnenko equation

Zhang Min, Ma Yu-Lan, Li Bang-Qing
Chin. Phys. B . 2013, 22(3): 030511. **doi:** 10.1088/1674-1056/22/3/030511

One-dimensional mass transport with dynamic external potentials*

Xingxing Zhang(张星星), Dongqin Zheng(郑冬琴)†, and Weirong Zhong(钟伟荣)‡

Siyuan Laboratory, Department of Physics, Jinan University, Guangzhou 510632, *China*

(Received 1 November 2018; revised manuscript received 12 December 2018; published online 10 January 2019)

Using non-equilibrium molecular dynamics and the Monte Carlo method, we simulated mass transport in a one-dimensional channel with dynamic external potentials. This study focuses on the influence of the dynamic external potential field on the mass transport. Traveling wave and standing wave potential fields have been employed as our dynamic potential field. We found that mass transport can be promoted by the traveling wave field when the external potential moves along the direction of the mass current. When the standing wave field is exerted on the channel, the channel is found to work like a switch. The mass current can be "on" or "off" by adjusting the standing wave frequency. The effects of the period number, the amplitude and the velocity of the external potential on the mass transport are also discussed. Our research provides valuable advice for the control o particle transport through one-dimensional channels.

Keywords: dynamic external potentials, traveling wave, standing wave, mass transport

PACS: 05.60.Cd, 66.10.cg, 47.60.Dx, 47.61.–k **DOI:** 10.1088/1674-1056/28/2/020505

1. Introduction

Studies of mass diffusion and transport in low dimensional systems play an important role in the field of nanofluidics, especially with the discovery of low dimensional materials, such as carbon nanotube and graphene.[1–3] Researchers have been able to find some special characteristics of mass transport in low dimensions,[4,5] or some ways to control the transport.[6,7]

In previous studies, some basic properties of fluids have been derived. The equilibrium adsorption and surface properties in one[8] or two[9] dimensional pores have successfully been predicted using a weighted density functional theory. The ion density distributions and partitions in a charged cylindrical pore were investigated using a partially perturbative density functional theory based on the modified fundamental measure theory.[10] The expression of the effect of interparticle potential on nanofluids was derived by mathematical methods.[11] The dynamic separation factors and equilibrium selectivity of Lennard–Jones particles and their mixture in two-dimensional pores were studied using grand canonical Monte Carlo and molecular dynamics simulations.[12] In the process of studying the fluid properties, an external potential is found to be able to influence the diffusion or transport behavior of fluid. Studies of Brownian particles moving in a periodic potential have been done and the diffusion state has been obtained.[13] The invariability of particle transport velocity,[14] peak value,[15] the locked-to-running transition,[16] and retardation or promotion characteristics[5] under different potential field conditions have been discussed. In addition, particle transport rate under the deformation potential fields has also been studied.[17]

In addition to studies that used static external potentials, a dynamic external potential field can be used to control mass transport due to its dynamic mode and speed controllability. In previous studies, the enhanced diffusion with noise modulation under the fast moving period potential has been achieved.[18] Later, diffusion anomalies in ac driven Brownian ratchets were discovered.[19] In fact, dynamic potential can be defined as a driving force that changes with time, which means that this type of research can appear in many forms. Rakesh *et al.*[20] mimicked the effects of periodically moving external potential on particle transport through a moving defect site. They found that the most efficient transport can be achieved in either direction along the ring. Bandyopadhyay *et al.*[21] previously analyzed the dependence of Brownian particles on frequency and space in the periodic potential field by numerical calculation. Sandor *et al.*[22] studied the process from strong coupling to complete separation for active matter run-and-tumble disk systems on a traveling-wave substrate. Benichou *et al.*[23] analyzed the negative differential migration between particle velocity and applied force in crowded environment. These studies show some of the possibilities of applying dynamic external potential to realize transport controlling or particle separation. However, more research in this area is worthwhile.

Most researchers design their dynamic potential in the form of a traveling-wave. In this paper, we construct two types of dynamic potentials: traveling wave and standing wave potential. They are applied on a non-equilibrium particle system in one dimension.[24,25] The mass transport under the potentials is simulated by molecular dynamics method, which is based on the statistical mechanics.[26] The major goal of our

*Project supported by the Natural Science Foundation of Guangdong Province, China (Grant No. 2014A030313367).

†Corresponding author. E-mail: zhengdq@jnu.edu.cn

‡Corresponding author. E-mail: wrzhong@hotmail.com

© 2019 Chinese Physical Society and IOP Publishing Ltd

research is to find if the dynamic potentials influence the mass transport behavior, and thus provide insights on the possibility of realizing mass transport control by using dynamic external potentials.

2. Models and methods

The model used in this paper, as shown in Fig. 1, consists of three parts: a high concentration particle reservoir (the green balls on the left side), a low concentration particle reservoir (the blue balls on the right side), and a particle transport channel (the middle part between the two reservoirs). During the process of simulation, the particle reservoir maintains a relative constant particle number. The lengths of the two reservoirs are $L_{\rm l}$ and $L_{\rm r}$, while $N_{\rm l}$ and $N_{\rm r}$ are the particle numbers in them, respectively. Two types of dynamic external potentials are exerted on the particle channel: the traveling wave and standing wave potential, as shown in Fig. 1(a) and Fig. 1(b), respectively. The arrows in Fig. 1 represent the moving directions of the potential fields.

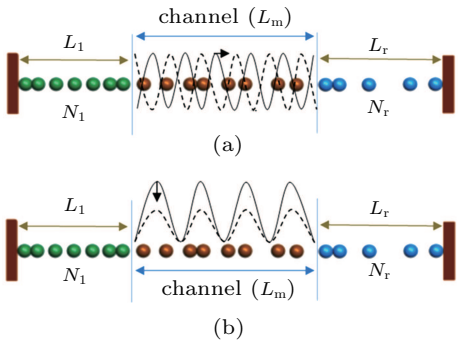


Fig. 1. One-dimensional model for dynamic external potentials: (a) traveling wave channel model, (b) standing wave channel model. The solid and dashed lines represent the waveform of the external potential field at two different moments, respectively.

In Fig. 1(a), the solid line and dashed line respectively represent the waveform of the external potential field at two different moments for the traveling wave channel. It can be seen that the field moves along the particle channel, and the field shape and amplitude are fixed, which is similar to the travelling wave. The motion pattern of standing wave channel is given in Fig. 1(b). The potential does not move along the channel but its amplitude changes in a cyclical manner, which is similar to the half standing wave. The potentials of the two motion patterns described above are given by the following equations:

$$U_{\rm t}(x,t) = U_{\rm n}\cos\omega\left(t-\frac{x}{v}\right), \tag{1}$$

$$U_{\rm s}(x,t) = U_{\rm m}\cos^2(\pi f t)\sin^2\frac{\pi x}{\lambda}, \tag{2}$$

where $U_{\rm t}(x,t)$, $U_{\rm s}(x,t)$ represent the traveling wave and standing wave potential, respectively, and x and t represent the position and time. $U_{\rm n}$ and $U_{\rm m}$ are the amplitude of the corresponding potential field. $\omega = 2\pi/T_0$, is the angular velocity, in which T_0 is the motion period of the potential field. v is the traveling wave velocity. f is the standing wave frequency. $\lambda = (x_{\rm r}-x_{\rm l})/n_{\rm f}$, is the wavelength of the potential field function, in which $n_{\rm f}$ is the number of spatial cycles of the potential field in the range of particle channel, and $x_{\rm l}$ and $x_{\rm r}$ are the coordinates of the left and right endpoints of the channel.

The particle transport process is simulated by molecular dynamics method. The interaction between particles is described by the Lennard–Jones (LJ) potential. The temperature of the system is controlled by Langevin heat baths.[27] The calculation process involved in the molecular dynamics method is realized by Verlet algorithm, and the time step is 0.55 fs.[28] Particles are subjected to two kinds of force in the process of passing through the channel. One is the interaction force between the particles due to the LJ potential, and the other is the force coming from the external potential. The comprehensive effect of these forces will eventually affect the transport behavior of particles.

In the simulation, we control the number of particles in the left and right reservoirs by the Monte Carlo method. The specific algorithm refers to Metropolis calculation method. The particle number in the reservoir is set as N. When the number of particle in the reservoir is less than N, the system will generate a new particle. A random position and initial velocity are given to this new particle. The probability that the particle will be accepted is

$$P_{\rm cr} = \min\left[1, \exp\left(-\frac{\Delta U}{kT}\right)\right], \tag{3}$$

where k is the Boltzmann constant, T is the temperature of the particle reservoirs, and ΔU is the variation of the system potential energy after adding this particle. If $\Delta U \le 0$, the acceptance probability is 1, which means the particle generated at this time can be fully accepted. If $\Delta U > 0$, its acceptance probability $P_{\rm cr} = \exp(-\Delta U/kT)$. A random number P in the range between 0 to 1 is generated. If $P_{\rm cr} \ge P$, the generated particle can be accepted, otherwise, the behavior of generating the particle is invalid, and the number of particle in the reservoir remains unchanged.

When the number of particles in the reservoirs is greater than N, the system randomly selects a particle that may be deleted, and the deletion probability is

$$P_{\rm de} = \min\left[1, \exp\left(-\frac{\Delta U}{kT}\right)\right]. \tag{4}$$

The specific method is similar to the process of adding particles.

The interaction between particles is expressed by the LJ potential function

$$U(r) = 4\varepsilon\left[\left(\frac{\sigma}{r}\right)^{12} - \left(\frac{\sigma}{r}\right)^{6}\right], \tag{5}$$

where r is the distance between particles, ε and σ, which depend on the type of particles, are potential parameters. The

magnitude of ε reflects the depth of the potential function curve, and σ reflects the equilibrium distance between particles. In this potential function, $(\sigma/r)^{12}$ describes the repulsive term and $(\sigma/r)^6$ describes the attraction term, respectively.

Langevin heat bath controls the temperature of the system. The equation of motion is described as

$$m_i \frac{\mathrm{d}^2 x_i}{\mathrm{d}t^2} = -\frac{\partial U_i(x)}{\partial x_i} - m_i \zeta_i \frac{\mathrm{d}x_i}{\mathrm{d}t} + R_i(t), \tag{6}$$

where m is the particle mass, x is the position vector, and ζ is the friction coefficient. $R_i(t)$ is the random force with zero mean and variance of $2m_i\zeta_i K_\mathrm{B} T_0$, of which denotes the independent Wiener process. $U_i(x)$ represents the sum of the external potential field and the LJ potential between particles.

For convenience of description, dimensionless processes are taken for all the physical quantities involved in the model. The specific formulas are as follows: the length is $L^* = L/\sigma_0$, the temperature is $T^* = T/\varepsilon_0$, the concentration is $c^* = c\sigma_0$, the potential parameters are $\varepsilon^* = \varepsilon/\varepsilon_0$ and $\sigma^* = \sigma/\sigma_0$, the average velocity is $\bar{v}^* = \bar{v}(m_0/\varepsilon_0 k)^{1/2}$, the potential is $U^* = U/\varepsilon_0 k$, the mass flux is $J^* = J\sigma_0(m_0/\varepsilon_0 k)^{1/2}$, the frequency is $f^* = f\sigma_0/(m_0/\varepsilon_0 k)^{1/2}$. In these formulas k is the Boltzmann's constant, m_0 is 1/12 mass of carbon atoms, σ_0 and ε_0 are the LJ potential parameters of the helium atom, $\sigma_0 = 0.258$ nm, $\varepsilon_0 = 10.22$ K. The particle mass m used in our model is the relative atom mass.

3. Results and discussion

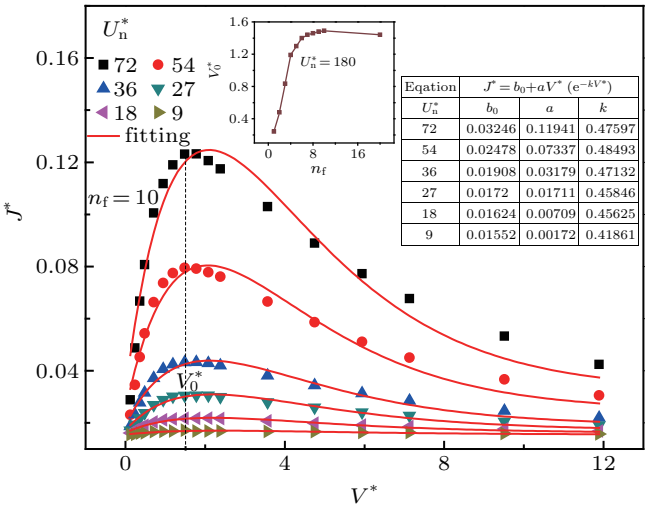
3.1. Traveling wave channel

To study the effect of the potential moving along two directions of the channel on particle transport, we take the direction from high to low concentration as a positive direction, and on the contrary as negative. Figure 2 shows the relationship between the particle current through the channel and the parameters of the traveling wave potential, including the amplitude, the number of periods, and the velocity of the traveling wave potential. It can be seen that when the potential moves along the positive direction, the particle current is enhanced significantly. The particle current has a maximum value in the positive direction, and the corresponding potential velocity is defined as the optimal velocity V_0^*. For the same period number n_f, V_0^* does not change with the amplitude of the potential. The inset of Fig. 2 shows that V_0^* increases with n_f. When n_f is larger than 10, the optimal velocity does not change. This happens because when a particle passes through the channel, the force exerted by the external potential field is positive–negative alternating. Both of the positive and negative force will influence the particle current. If the potential moves in the positive direction, then it can provide a driven force to the particle at most of the time, just like we swallow food, so the particle current increases obviously. Furthermore, as the potential moves faster and faster, the particle cannot keep up with it and then the particle current will decrease.

To reach a quantitative analysis, we make the fitting according to the feature of the curve in Fig. 2. It is found that the dependence of particle current J^* on traveling wave velocity V^* can be fitted by the Maxwell-like formula:

$$J^* = b_0 + aV^* \left(\mathrm{e}^{-kV^*}\right). \tag{7}$$

The solid lines in Fig. 2 show the fitting results, In our model, the particle coupling to heat baths which obey Maxwell–Boltzmann distribution, then there is a most probable velocity for all particles. Thus, when the travelling velocity matches the most probable velocity of particles, the driven force will reach maximum and the particle current has a maximum value in the positive direction.



Eqation	$J^*=b_0+aV^*\,(\mathrm{e}^{-kV^*})$		
U_n^*	b_0	a	k
72	0.03246	0.11941	0.47597
54	0.02478	0.07337	0.48493
36	0.01908	0.03179	0.47132
27	0.0172	0.01711	0.45846
18	0.01624	0.00709	0.45625
9	0.01552	0.00172	0.41861

Fig. 2. Particle current depends on the traveling wave velocity of the channel. The inset shows the n_f dependence of optimal traveling wave velocity. The concentration difference between the left and right particle reservoirs is 0.57.

We studied the effect of traveling wave field on mass transport at different concentration gradients, the results are shown in Fig. 3. The data shown in Fig. 3(a) are obtained when there is no concentration difference between the two reservoirs. We found that under the action of the traveling wave field, there exists a directional particle current, even if there is no concentration difference between the left and right particle reservoirs. The relationship between particle current and traveling wave velocity is similar to that in Fig. 2. The optimal velocity V_0^* of the potential field still exists, but the corresponding V_0^* without concentration gradient is larger than that of Fig. 2. Figure 3(b) shows the variation of particle current with concentration gradient at different traveling wave velocity. It can be seen that the particle current increases linearly with the concentration gradient when the concentration gradient is small, and the effect of traveling wave velocity on parti-

cle transport is not obvious. As the concentration gradient increases, the increase rate of particle current decreases but the effect of traveling wave velocity on particle transport increases significantly. At a certain concentration gradient, the particle current increases at first and then decreases with the increase of velocity, which is consistent with the previous conclusion.

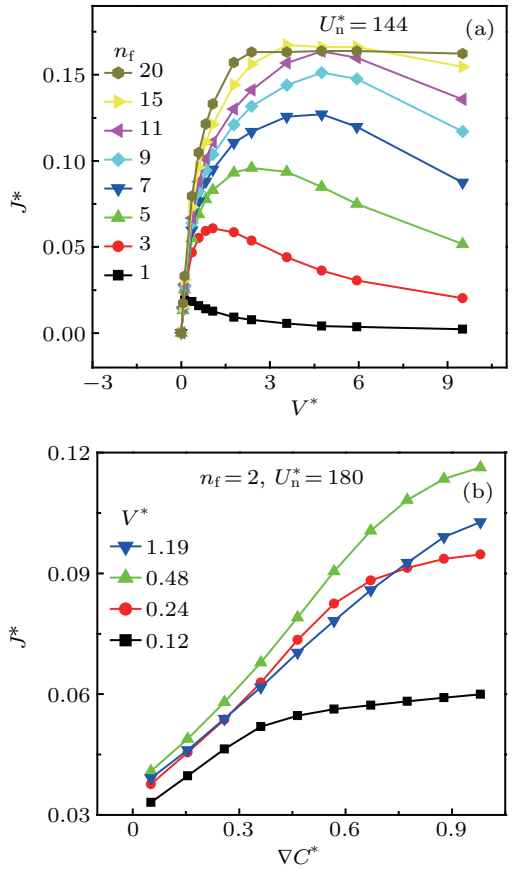


Fig. 3. Particle current depends on the traveling wave velocity (a) and the concentration gradient (b).

To understand this result, we analyze the distributions of the velocity and the concentration of the particles in the channel. Usually, particles are more likely to be concentrated in a local potential minimum for static potential,[29] so the distribution of particle density and velocity is not uniform under static potential. But the situation changes when the potential is dynamic. The distributions of particle density and velocity under dynamic potential field are given in Fig. 4. When $U_n^* = 18$, the particle density and velocity distribution conform to the law of diffusion transport. The particle density in the channel decreases gradually from the left-hand reservoir to the right-hand reservoir, while the velocity increases gradually. With the increase of the potential amplitude, the gradient of density and velocity at the channel boundary increases, but within the channel, the distribution tends to be uniform. This implies a gradual transition from diffusion transport to ballistic transport. When $U_n^* = 180$, ballistic transport is fully achieved. Under this situation, there is almost no collision between particles in the channel, and the particle density and velocity tend to be the same along the channel.

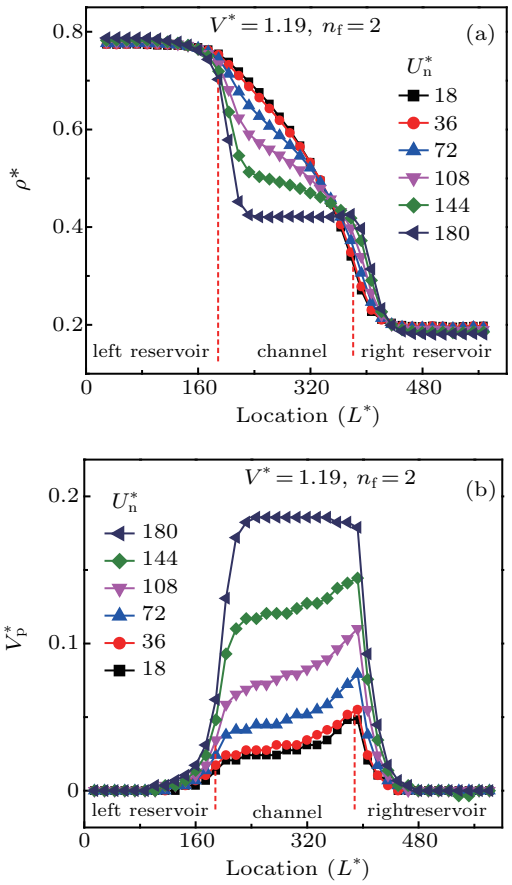


Fig. 4. Distribution of (a) particle density and (b) average velocity of the particle under traveling wave field.

3.2. Standing wave channel

In this section, we will show the effect of standing wave field on the mass transport. Figure 5(a) gives the dependence of particle current on the standing wave frequency and the amplitude of the external potential. We can see that the particle current decreases with the potential amplitude. When the potential amplitude is small, the particle current is almost independent of the standing wave frequency. However, when the amplitude is greater than 126, the standing wave frequency presents a switch effect on the particle current. Here, for convenience of description, we define the stable region with high particle current as the low frequency region, the frequency range with sharp variation of particle current as medium frequency region, and the stable region with lower particle current as high frequency region. The frequency point connecting the intermediate frequency region and the high frequency region is defined as the cutoff frequency. From Fig. 5(a), it can be seen that the cutoff frequency does not change with the amplitude of the external potential when n_f is fixed.

Figure 5(b) shows that the particle current almost does not change with n_f in high or low frequency area. The low frequency corresponds to large particle current, and the high frequency corresponds to small particle current. This result is

consistent with Fig. 5(a). For the frequency between 140 and 5.5×10^3, the particle current increases with n_f, and finally reaches saturation. The saturated current is dependent on the frequency. Figure 5(c) describes the effect of frequency and n_f on particle current from another perspective. It can be seen that n_f may influence the cutoff frequency. Although n_f does not change the particle currents in the low and high frequency region, it changes the conversion point. The cutoff frequency increases with the n_f.

To explain this phenomena, we tried to give the trajectories of the particles in the channel. The n_f is chosen as 2, so there is a potential well in the middle of the channel. On either side of the potential well is a potential barrier. A particle has to pass through the two barriers to get to the other side of the channel. The particle trajectories under different external potential frequencies are given in Fig. 6. From Fig. 6(a) it can be seen that when the frequency is low, the particles pass through the channel almost without stopping. While when the frequency becomes medium (see Fig. 6(b)), the particles will stay in the potential well for a long time, which means that the probability for the particle passing through the barrier decreases. When the frequency reaches the high frequency region (see Fig. 6(c)), the probability of passing through the barrier is almost zero. This result may give an insight into the mechanism that how the external potential field influences the particle current. Our research model is similar to the literature,[30] both of which are driven by external forces to produce a directed mass flux with frequency dependence. However, the specific physical mechanism is somewhat different, which is attributed to the fact that standing wave in our study could not propagate forward like the mechanical vibrating in Ref. [30] and generate the differences in the phase and decay between the two waves. In addition, there is no obvious resonance region in our research.

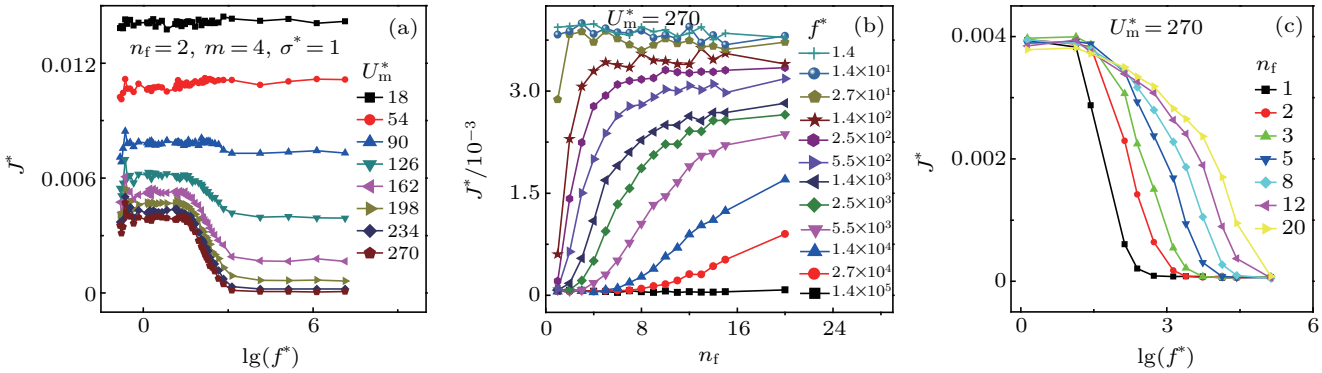


Fig. 5. Effect of standing wave field on particle current. (a) Frequency dependence of particle current for different potential amplitudes, (b) the variation of particle current with n_f at different standing wave frequencies, (c) the frequency dependence of particle current for different n_f.

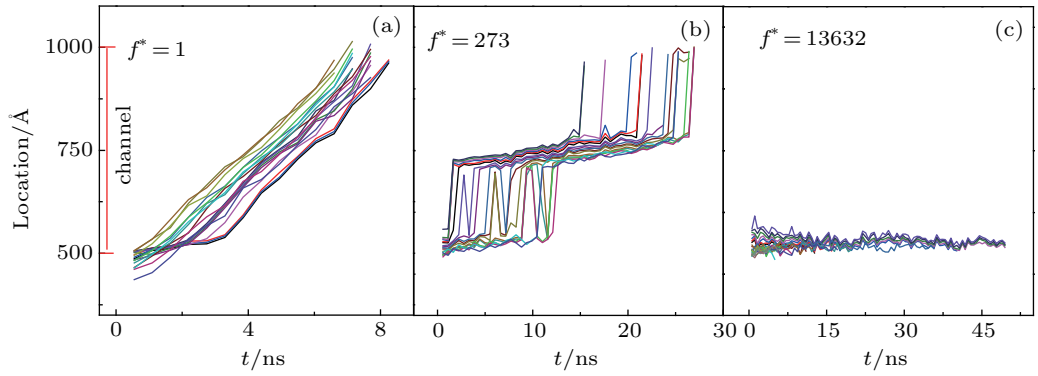


Fig. 6. Particle trajectory tracking with $U_m^* = 270$ and $n_f = 2$ under $f^* = 1$ (a), $f^* = 273$ (b), and $f^* = 13632$ (c). The line distinguished by color in each figure represents the trajectory of a particle.

In addition, to study the transport performance of different kinds of particles in the standing wave channel, we changed the values of particle mass m and LJ parameters σ^* in order to understand the effects of particle mass and size on particle transport. As shown in Fig. 7, with the increase of particle mass or σ^* value, the particle current shows an overall downward trend. The common feature is similar to that of Fig. 5. The curve of particle current with frequency can be divided into three regions: low, medium and high frequency. In the medium frequency region, the particle current drops sharply, which exhibits the switch characteristics of the standing wave frequency to the particle current. The cutoff frequencies are different for different mass and σ^*, which means that different types of particles have different cutoff frequencies. This result provides possibility for realizing particle filtration by controlling the standing wave frequency.

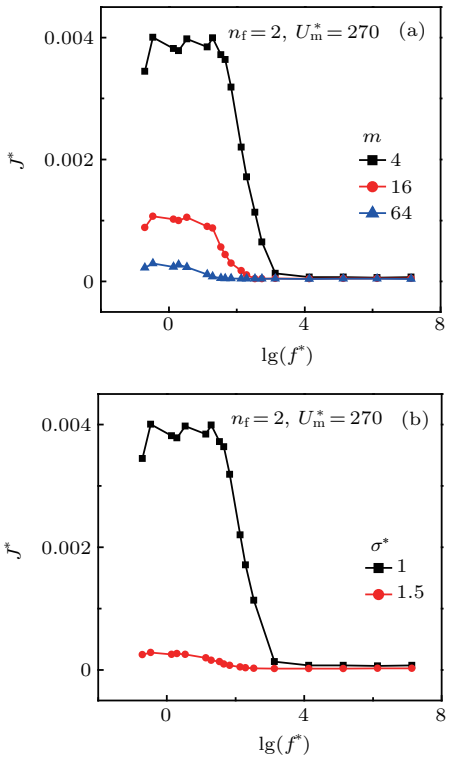


Fig. 7. Frequency dependence of particle current for different parameters: (a) mass m, (b) LJ potential parameter σ^*.

4. Conclusion

We used the molecular dynamics and Monte Carlo method to study the transport performance of particle channel with traveling wave and standing wave potential field. Our results show that the positive traveling wave velocity is helpful for the particle transport. There is an optimal traveling wave velocity in the positive direction, at which the particle current reaches the maximum value. The optimum velocity is related to the period number of potential, but is not affected by the amplitude of potential.

For the standing wave channel, the standing wave frequency presents a switch effect to the particle current. When the frequency is low, the particle current is large, and the channel is "on", while when the frequency is high, the particle current is small, and the channel is "off". The cutoff frequency is independent of the amplitude of the external potential, but is related to the periodic number of the potential field n_f. When n_f is larger, the cutoff frequency is also larger. The particle mass and the LJ potential parameter σ^* also affect the cutoff frequency. When value of the mass or σ^* is larger, the cutoff frequency will be lower.

Finally, we would like to emphasize the practical implications of this work. The study presented in this paper gives an insight into the potential relationship between particle transport with the motion mode of the external potential. The parameters that enter the potential can be used to separate different species of particles and control the particle transport rates. These results provide some references for controlling or filtering mass transportation.[31] This study is helpful for designing nanofluidic device, or provide some new thoughts on the study about fluid movement in porous media. In addition to applications mentioned earlier, it can also be an analogy to the simplified movement pattern of biological ion channels with potential field,[32–34] which also provides some insights for the research of biological ion channels.

Acknowledgment

We would like to pass on our thanks to the high performance computing platform of Jinan University and Siyuan Clusters for providing computing resources.

References

[1] Brennan M E, Coleman J N, Panhuis M I H, Marty L, Byrne H J and Blau W J 2001 *Synth. Met.* **119** 641
[2] Wen J L, Zheng D Q and Zhong W R 2015 *Rsc Adv.* **5** 99573
[3] Pan H, Li J Y and Feng Y P 2010 *Nanoscale Res. Lett.* **5** 654
[4] Chen P R, Xu Z C, Gu Y and Zhong W R 2016 *Chin. Phys. B* **25** 086601
[5] He J h, Wen J L, Chen P R, Zheng D Q and Zhong W R 2017 *Chin. Phys. B* **26** 070502
[6] Zhou X Y, Wu F M, Kou J L, Nie X C, Liu Y and Lu H J 2013 *J. Phys. Chem. B* **117** 11681
[7] Shen L, Xu Z, Zhou Z W and Hu G H 2014 *Chin. Phys. B* **23** 118201
[8] Peng B and Yu Y X 2008 *Langmuir* **24** 12431
[9] Yu Y X and Wu J 2003 *J. Chem. Phys.* **119** 2288
[10] Xin Y, Zheng Y X and Yu Y X 2016 *Mol. Phys.* **114** 2328
[11] Sun M H and Zhang X R 2018 *Int. J. Heat Mass Transfer* **122** 150
[12] Wang S M, Yu Y X and Gao G H 2006 *J. Membr. Sci.* **271** 140
[13] Pavliotis G A and Vogiannou A 2008 *Fluct. Noise Lett.* **8** L155
[14] Lindenberg K, Sancho J M, Lacasta A M and Sokolov I M 2007 *Phys. Rev. Lett.* **98** 020602
[15] Wang F, Deng C, Tu Z and Ma H 2013 *Acta Phys. Sin.* **62** 040501 (in Chinese)
[16] Bai Z W and Zhang W 2018 *Chem. Phys.* **500** 62
[17] Mbemmo A M F, Kenmoe G D and Kofane T C 2017 *Fluct. Noise Lett.* **16** 1750011
[18] Spagnolo B and Dubkov A 2006 *Eur. Phys. J. B* **50** 299
[19] Spiechowicz J and Luczka J 2015 *Phys. Rev. E* **91** 062104
[20] Chatterjee R, Chatterjee S, Pradhan P and Manna S S 2014 *Phys. Rev. E* **89** 022138
[21] Bandyopadhyay M, Dattagupta S and Sanyal M 2006 *Phys. Rev. E* **73** 051108
[22] Sandor C, Libal A, Reichhardt C and Reichhardt C J O 2017 *Phys. Rev. E* **95** 012607
[23] Benichou O, Illien P, Oshanin G, Sarracino A and Voituriez R 2014 *Phys. Rev. Lett.* **113** 268002
[24] Marconi U M B, Puglisi A, Rondoni L and Vulpiani A 2008 *Phys. Rep.* **461** 111
[25] Seifert U 2012 *Rep. Prog. Phys.* **75** 126001
[26] Chou T, Mallick K and Zia R K P 2011 *Rep. Prog. Phys.* **74** 116601
[27] Chetrite R, Falkovich G and Gawedzki K 2008 *J. Stat. Mech.* P08005
[28] Gmachowski L 2018 *Eur. Biophys. J.* **47** 309
[29] Lindner B and Sokolov I M 2016 *Phys. Rev. E* **93** 042106
[30] Zhou X Y, Wu F M, Liu Y, Kou J L, Lu H and Lu H J 2015 *Phys. Rev. E* **92** 053017
[31] Dunlop J, Bowlby M, Peri R, Vasilyev D and Arias R 2008 *Nat. Rev. Drug Disc.* **7** 358
[32] Allena T W, Bliznyuk A, Rendell A P, Kuyucak S and Chung S H 2000 *J. Chem. Phys.* **112** 8191
[33] Mashl R J, Tang Y Z, Schnitzer J and Jakobsson E 2001 *Biophys. J.* **81** 2473
[34] Oh Y, Kim J, Yethiraj A and Sung B J 2016 *Phys. Rev. E* **93** 012409